Expression of Concern

An Efficient Model for Detection and Classification of Internal Eye Diseases using Deep Learning

Richa Gupta; Vikas Tripathi; Amit Gupta

2021 International Conference on Computational Performance Evaluation (ComPE)

10.1109/ComPE53109.2021.9752188

This is a temporary expression of concern. After publication, IEEE learned that the article contains tortured, or nonsensical, phrases which may impact the reliability of the results. The article is under investigation by a duly constituted expert committee and this note will remain appended to the article until the review process is complete.

2021 International Conference on Computational Performance Evaluation
(ComPE) North-Eastern Hill University, Shillong, Meghalaya, India. Dec 1-3, 2021

An Efficient Model for Detection and Classification of Internal Eye Diseases using Deep Learning

Richa Gupta
Department of CSE
Graphic Era Deemed to be University
Dehradun, India
richa1883gupta@gmail.com

Vikas Tripathi
Department of CSE
Graphic Era Deemed to be University
Dehradun, India
vikastripathi.be@gmail.com

Amit Gupta
Department of CSE
Graphic Era Hill University
Dehradun, India
amitgupta7920@gmail.com

2021 International Conference on Computational Performance Evaluation (ComPE) | 978-1-6654-3656-4/21/$31.00 ©2021 IEEE | DOI: 10.1109/ComPE53109.2021.9752188

***Abstract*— Natural eye is influenced by the distinctive eye illnesses some of them are great cause of vision loss. Many Artificial Intelligence (AI) approaches have been proposed for the identification of such diseases. The proposed method intends to plan an AI based automated network for eye illness identification and grouping to help the ophthalmologists all the more viably distinguishing and ordering of internal eye diseases like Choroid Neovascularisation (CNV), Diabetic Macular Edema (DME) and Drusen by utilizing the Optical Coherence Tomography (OCT) pictures portraying various tissues. The procedure utilized for planning this framework includes diverse deep learning convolutional neural organization (CNN) models. The proposed methodology is called efficient because it is performed on a large scale data-set which has four classes and improves the performance to a great level. The best picture subtitling model is chosen after execution investigation by looking at different picture inscribing frameworks for helping ophthalmologists to identify and order eye illnesses. The proposed methodology achieves the performance to a great level, 83.66% of accuracy for the test images when the data-set is divide in the format of 70-30 ratio.**

Keywords*— Deep Learning, VGG-16, CNV, DME, Drusen, OCT

I. INTRODUCTION

In health care system Artificial intelligence (AI) using Deep Learning (DL) is a great innovation. In ophthalmology, for detection and classification of different eye diseases with the help of retinal mages like optical coherence Tomography (OCT) and Fundus images, AI and DL become more popular because of their efficiency and high speed [1]. In this paper eye diseases are identified in OCT images using a DL model. Human eye has a complex structure which has many intrinsic parts such as cornea, iris, pupil, lens, retina, macula, optic nerve and vitreous. Any of these parts can have some problem which may lead to an eye disease. The eye diseases can be classified into two categories internal and external.

A. Internal eye diseases

Many eye illnesses have no early indications. They might be easy, and you may see no adjustment in your vision until the illness has gotten very progressed. Some of the internal eye diseases are AMD, Cataracts, CMV Retinitis, Color blindness, DME, Glaucoma, keratoconus, Ocular hypertension, Uveitis, CNV and Drusen. In this work three internal eye diseases CNV, DME and Drusen are identified and theses all are related to AMD.

B. External eye diseases

Since the outside of the eye is in direct contact with the climate, it is powerless to diseases and wounds. There are additionally various genetic sicknesses that can affect the external eye. The significant indications of outer eye illness are redness that doesn't improve with treatment and helpless vision not clarified by retina issues. Some external eye diseases are Pink Eye, Corneal Abrasion, Cornea Abnormalities, Acanthamoeba keratitis, Conjunctivitis, Dry eye, Excessive tearing, Keratitis, Photokeratitis, Presbyopia (age-related farsightedness), nearsightedness, farsightedness, and astigmatism**.**

OCT images plays a critical role in ophthalmology because it gives an insight to the internal condition of the retina. In OCT images the high-resolution image of the biological tissue is taken with the help of coherent light. It takes the cross-sectional image of retina from 30 to 40 degree of angle. Thus, this image is utilized to identify any kind of eye diseases related to retina. These images can be easily interpretable. In this work OCT images are used for the disease detection like CNV, DME and Drusen. Sample input images of different classes are shown in fig-1.

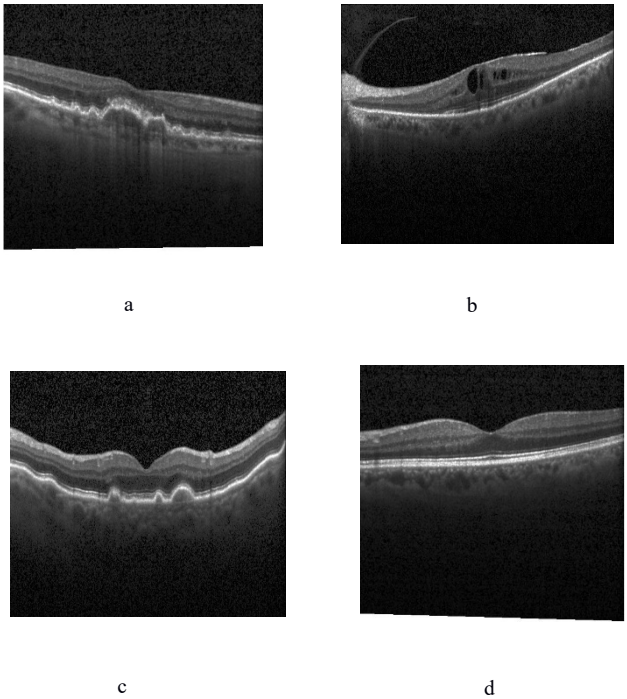

Fig-1 Sample input images (a)CNV (b)DME (c)Drusen (d)Normal

DR is the major cause for the damage of the small blood vessels. Macula and the retina is infected because of the leakage of the fluid. In diabetic patients DME is very common disease which may lead to the vision loss. AMD is

the disease which is because of the changes happened in the Macula due to age. AMD is divided into the two categories early and late AMD. The changes occur between the retina and choroid is referred to as Drusen. If Drusen is detected then the Early AMD is also can be identified. The macular degeneration and aging is the root of the Drusen. In Drusen the vision is blurred. Early AMD can be detected easily if the patient has Drusen. CNV is the disease where new vessels produced automatically in the choroid. Late AMD can be detected through CNV.

In DL many Neural Networks have been developed which perform outstanding for the disease detection. In this paper a DL model called VGG-16 is utilized for the classification and detection of the diseases.

Visual Geometric Group called VGG developed at Oxford university. It is combination of 16 layers. Each layer contains trainable parameters and some other layers do not have any parameters which are trainable [24].

VGG has a number of versions start from VGG-11 to VGG-19. Primary classification and identification are greatly affected by the depth of the convolutional networks. VGG-11 has 11 layers, 8 convolutional (CV) layers and 3 fully connected (FC) layers and VGG-19 has 19 layers, 16 CV and 3 FC layers. All the versions of VGG have same 5 blocks of CV followed by Max Pool layer and all has same 3 FC antipodal, the only difference is the number of interconnected CV are added in the five blocks of CV.

The followed sections of the paper described as Section 2 includes the related work that has been carried out till date. Section 3 describes the proposed methodology. Section 4 is the discussion of the result of the model, section 5 is the comparison of proposed method to a previous work and the last section is the conclusion for the paper.

II. Related Work

An automatic model for Micro aneurysms (Mas) detection and new contrast normalization techniques is introduced by Alan D. Fleming Et. Al. [1]. Method which utilizes the watershed method gives higher accuracy. The sensitivity of the proposed model is 85.4% and the specificity is 83.1%.

Optic circle (OD) location is a significant advance in creating frameworks for computerized finding of different genuine ophthalmic pathologies proposed by Arturo Aquino Et.Al [2]. The work shows another format-based method for OD division by methods for a roundabout OD-limit estimate. For finding the OD position needed by calculations, new OD philosophy is introduced. OD divisions are efficiently detected by the proposed model.

Gwenole Quellec Et.Al [3] proposed an automated model for the identification of diseases like microaneurysms, the primary symptom of DR, and the recognition of drusen, the sign of AMD. In proposed work an overall structure for distinguishing and portraying objective injuries promptly. This system depends on a component space consequently got from a bunch of reference picture tests speaking to target injuries, including atypical objective sores. Factor examination is utilized to infer the channels creating this component space from the tests. Beforehand concealed picture tests are then characterized in this component space. We tried this methodology via preparing it to identify microaneurysms. On a bunch of pictures from 2739 patients incorporating 67 with referable DR, DR discovery region under the recipient working trademark bend (AUC) was tantamount to our recently distributed red injury identification calculation. We additionally tried the methodology on the location of AMD, via preparing it to separate drusen from Stargate's sickness injuries, and accomplished an AUC = 0 850 on a bunch of 300 physically recognized drusen and 300 physically distinguished specks.

Peripapillary decay (PPA) is a decay of prior retina tissue. Due to its relationship with eye illnesses, for example, near-sightedness and glaucoma, PPA is a significant marker for determination of these infections. Jun Cheng Et.Al. [4] used a central district is fragmented using the retina images and the BIF is separated. As BIF is a naturally an element inserted into a higher dimension space, it isn't reasonable to gauge the comparability between two BIFs straightforwardly dependent on the Euclidean separation. Accordingly, it is important to get a reasonable planning to decrease the size of dimensions. This model investigates meagre exchange figuring out how to move the mark data from clinicians to the example dissemination information accommodate in all examples. Particular grouping investigation is utilized to characterize two procedures of meagre exchange learning: negative and positive inadequate exchange learning. Trial output demonstrate that the negative meagre exchange learning is better than the positive one for this assignment. BIF based methodology accomplishes a precision of over 90% in identifying PPA, obviously superior to past strategies.

An optic plate and optic cup division technique utilizing super pixel characterization for glaucoma screening by Jun Cheng Et.Al. [5]. In optic circle division, histograms, and focus encompass insights are utilized to group each super pixel as plate or non-circle. A self-appraisal dependability record is registered to assess the nature of the mechanized optic plate division. The strategies may be utilized for division and glaucoma identification. One constraint of the prospective cup division is that the prepared classifier is marginally overwhelmed by cups with intermediate capacity, thus the prospective technique disparages the huge cups, although exaggerate the little cups when paleness isn't self-evident.

Uyen T. V. Nguyen Et.Al.[6] proposed a novel technique for detection of AV scratching appraisal. With the help of retinal picture, the vascular organization is extricated utilizing the multiscale line recognition technique. The hybrid point discovery technique is employed to restrict all AV crossing areas. Then on every distinguished hybrid mark, 4 vessel fragments, two related to corridor and 2 related along the vessel, are distinguished and two venular sections perceived from the supply route vessel order strategy. The size of the vessel is determined and dissected to process the AV scratching seriousness of that hybrid. The trial results show a solid relationship between the figured AV scratching esteems and the master reviewing with a Spearman connection coefficient of 0.70. Affectability was 77% and particularity was 92% when looking at AV scratching identified utilizing the technique to that recognized utilizing the traditional method, implemented via prepared photographic graders.

Diseases like Referable DR and glaucomatous optic neuropathy are detected by implementing the CNN deep learning models by Stuart Et.Al [7]. Visualization regions of the fundus is the outcome of the model. The model is trained in groups and one group contain 100 images so a smaller number of images are analyzed so the model is biased in nature. New automated tools can be designed for the assistant of the medical persons in near future.

Artificial intelligence (AI) methods are discussed in Ursula Schmidt-Erfurth Hrvoje Bogunović [8] paper for the diagnosis process of abnormalities in human eyes. Almost all macular and retinal diseases are identified using AI and DL techniques. The efficiency of CNN is almost same as the specialist diagnosis so the acceptance of these ANNs are very popular in the field of medical. Diabetic retinopathy (DR) is detected efficiently with the help of AI automated models. Ophthalmology is highly empowered by the AI models for identification and therapies of the retinal diseases.

DeepSeeNet used in a model for classification of AREDS using bilateral CFP by Yifan Peng Et.Al. [9]. Total 58402 images are trained and 900 images are tested. Labels are gained by centre grades. Pigmentary abnormalities and drusen size are detected first then the severity is calculated. DeepSeeNet efficiently classify the abnormalities and the AUC is 94% for drusen eyes and 97% for AMD and 93% for pigmentary abnormalities.

An attention-based CNN for glaucoma location is designed, termed as AGCNN is proposed by Liu Li Et.Al. [10]. Total 11760 images are used for training purpose in which 4878 images contain glaucoma and 6882 images do not have glaucoma. Another structure of AG-CNN is planned, with a consideration forecast subnet, a neurotic zone limitation and a glaucoma arrangement subnet. The consideration maps are anticipated in the consideration expectation subnet to feature the striking districts for glaucoma recognition, under a feebly directed preparing way. Rather than alternative CNN strategies, the highlights are additionally envisioned as the restricted obsessive territory, which are additionally included AGCNN structure to upgrade the glaucoma identification execution. At long last, the investigation comes about because of testing over the LAG information base and the other glaucoma information base illustrate that the prospective AG-CNN approach essentially progresses the best in class in glaucoma location. AG-CNN gives the exactness 96.2%. the primary restriction of this model is that different fundus illnesses marginally impact the exactness of glaucoma location. New profound learning techniques can be conveyed in future.

Myopia which is a visual tissue causing visual disability stated by Xue-Bi Cai [11]. Near sightedness displays clear familial collection, and numerous confirmations have demonstrated that hereditary factors altogether add to its pathogenesis. Late sub-atomic innovations, for example, linkage investigation, up-and-comer quality validation, genome-wide affiliation study (GWAS), and cutting-edge sequencing (NGS) have distinguished numerous near sightedness related loci and hereditary transformations or variations. A superior comprehension of the hereditary premise setting off and controlling near sighted variation will additionally assist the near sightedness avoidance. the audit is to give a refreshed diagram of hereditary discoveries in non-syndromic near sightedness Studies worldwide have empowered basic advancement in understanding the hereditary premise of near sightedness since the time the primary exertion was made to disentangle its innate determinants during the 1960s. Helplessness qualities related with refractive blunder, pivotal length, and high near sightedness have been read for a long time, though hereditary affiliation concentrates on near sighted maculopathy have been restricted and warrant further turn of events. More broad investigations on extended transformation spectra, genotype-aggregate connections, novel quality recognizable proof, and organic portrayal new methods are required. The examinations may develop and broaden new comprehension of near sightedness hereditary qualities.

The advancement and the improvement of utilizing AI and DL innovation for DR identification just as momentum challenges in the genuine execution of DL models, and making an interpretation of DL examination into the medical field directly Carol Y. Cheung [12]. In outline, AI and DL are entering the standard of clinical medication. This innovation can enlarge specialist's knowledge to improve dynamic and operational cycles. Detecting DR is right around an ideal errand for AI in medical care. In future AI will get universal and imperative for the diagnosis process, with desire to enhance the proficiency and openness of diagnosis process, and consequently will have the option to keep visual misfortune and visual impairment from this overwhelming sickness.

An automated model for detection of difference in the corneal parameters due to age is build and find the relation with demographic factors, thus they can provide better results for detection of subclinical corneal ectasia (SCE). Cluster analysis were performed by JANELLE TONG Et.Al. [13] to recognize areas showing comparative varieties with age. The changes due to age were displayed utilizing polynomial relapse with sliding window strategies, and result of the method are checked with Bland Altman correlations. Pearson connections were applied to look at the effects of segment factors. Concentric group designs noticed for CT and FSSC however not for BSSC. Sliding window investigations provide good results for CT and FSSC/BSSC, individually.

In Muhammad Aamir Et.Al [14] Glaucoma is identified by using multi-level CNN in fundus images. The model has two phases, in first phase the glaucoma is detected and in second phase the disease is categorized into three level initial, medium and last. The model achieve the accuracy of 99.39%.

DR is detected in Thippa Reddy Gadekallu Et.Al [15] using Hybrid PCA DNN Model. DNN-PCA firefly model accuracy is 97% better than other models. Different metrices are calculated for the evaluation. The original dataset has the problem of over-fitting this is the basic limitation of the model. In future the same model can be employed to new data sets. AI based clinical choice emotionally supportive network for eye infection recognition and order to help the ophthalmologists all the more adequately recognizing and characterizing CNV, DME and drusen by utilizing the OCT pictures portraying various tissues is proposed by Sivamurugan Vellakani Et.Al [16]. The method utilized for planning this framework includes diverse D-CNN and long transient memory organizations (LSTM).

The best picture subtitling model is chosen after execution investigation by contrasting nine distinctive picture inscribing frameworks for helping the doctors to identify and

group eye illnesses. The important information investigation output acquired the models planned utilizing DenseNet201 with LSTM have prevalent execution regarding by and large precision of 96.9%, positive prescient estimation of 97.2 and genuine positive pace of 96.9 utilizing OCT pictures upgraded by the GAN.

III. PROPOSED METHODOLOGY

The proposed technique comprises of three significant steps specifically preparing, approval and testing the model. Picture inscribing model is utilized for producing inscriptions for OCT picture characterization. Deep scholarly VGG DL is utilized for include extraction. With a greater number of CV in CNN models, they can remove all the highlights compared to AI models.

In this work VGG-16 architecture is used to detect the internal eye diseases like CNV, DME and Drusen. For training a very rich dataset of 43293 images is utilized, thus, the training of the model is better than the previous method used.

The CNN model is prepared by utilizing fractional inscriptions to anticipate the following word in the grouping. This architecture is very simple to implement and for result analysis process. The overall structure of the proposed method is shown in Fig-2. As shown in Fig-2 this model consists 5 blocks of CV layers and at the end FC layers are placed. The model has 13 CV layers with 2 FC layers. The model has the input size of 224x224 images with 3 colors RGB. Each layer consists the parameters which are trainable and non-trainable. The FC layer with 6422784 merges to 1024 dimensions, this is so because the reduction of parameters.

As the layers passes the output to the next layers some changes in the parameters happed because of these changes some problem can be raise to decrease this kind of problem batch normalization is used. This normalization, normalize every layer's input and reduce the error rate and decrease the over fitting at some rate. Batch normalization improves the performance of the model.

Different dropout rate is applied to reduce the problem of over fitting.

Model checkpoint and early stopping is also included in the model. Check point monitor the specified matrices or parameter, in this model the validation accuracy is monitored thus the model is saved when it got highest validation accuracy.

Early stopping may stop the training of the model to the highest parameter value which is set to the model checkpoint if it is stable or decreasing

A. VGG-16

As visualized in Fig-3 VGG-16 has 5 blocks with convolutional layers followed by the Max-pooling layers, thus total 13 convolutional layers are there and 3 dense layers at the end. The dense layers are fully connected layers.

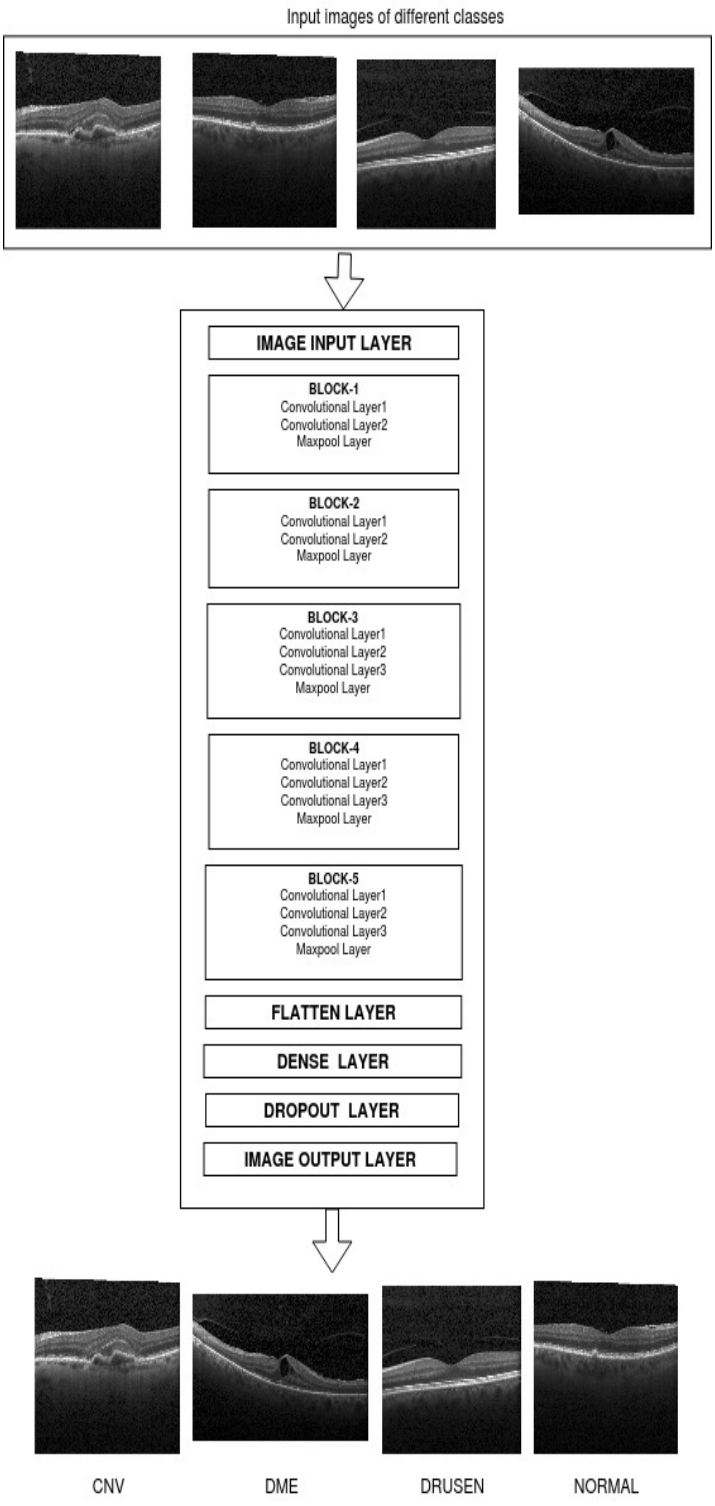

Fig-2 Architecture of Proposed method

Because there are 16 layers which has tunable parameters the model is called VGG-16. At the end a SoftMax layer is inserted which has 1000 outputs for each image. In VGG-16 the channel size starts with 64 and ends with 512, it is increased by a factor of 2.

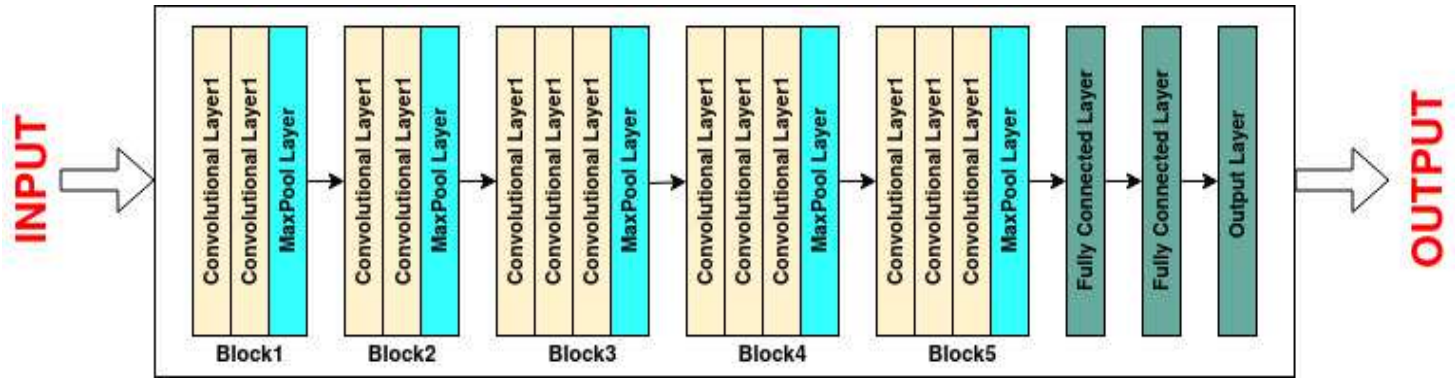

Fig-3 VGG-16 Flatten architecture

B. *Architecture of VGG-16 network*

1. Input Layer - In this layer the image of size 224 X 224 is fed with 3 channels red, green and blue
2. Convolutional Layer – after the input layer the images are passed through the convolutional layers which has a convolutional filter of 3 x 3 receptive field and stride of 1. Row and column padding is used by each convolutional kernel to maintain the size of input and output features.
3. Max Pooling Layer – These windows are non-overlapping and this operate on the 2 x2 max pool window with 2 strides.
4. Every block has a max pool layer at the end so few CV is succeeded by the max pool layer and some are followed by the convolutional layers itself.
5. FC layers have 4096 channels and the last output layer has 1000 channels.
6. The activation function used for the hidden layers is ReLU

Weights – Weights are downloaded from the image net dataset for the model.
Batch Size- 32 batch size is used for training purpose and for validation batch size is 10.

C. *Model Features*

VGG-16 model is used so 5 blocks are there with convolutional layers followed by the Max pool layer as illustrated in Fig-3. First 2 blocks have only 2 convolutional layers and the next 3 blocks consists 3 convolutional layers, at the end the 2 dense layers are used. In the model total number of parameters is 21,138,500 in which 6,423,812 are trainable parameters and 14,714,688 are non-trainable parameters. Model summary is given in Table I. The model detects and classified the diseases in the dataset. For making model deep this model utilized the FC layer and batch normalization to reduce the error rate and dropout for the over fitting problem.

D. *Activation function*

At first dense layer means FC layer ReLU activation function is applied and at the output layer the Soft max function is applied**.**

TABLE I CNN LAYERS DESCRIPTION

S. No.	Layer description	Image size with channel
1	Input Layer	224x224, 3
2	Convolutional2D Layer	224x224, 64
3	Convolutional2D Layer	224x224, 64
4	MaxPooling2D Layer	112x112, 64
5	Convolutional2D Layer	112x112, 128
6	Convolutional2D Layer	112x112, 128
7	MaxPooling2D Layer	56x56, 128
8	Convolutional2D Layer	56x56, 256
9	Convolutional2D Layer	56x56, 256
10	Convolutional2D Layer	56x56, 256
11	MaxPooling2D Layer	28x28, 256
12	Convolutional2D Layer	28x28, 512
13	Convolutional2D Layer	28x28, 512
14	Convolutional2D Layer	28x28, 512
15	MaxPooling2D Layer	14x14, 512
16	Convolutional2D Layer	14x14, 512
17	Convolutional2D Layer	14x14, 512
18	Convolutional2D Layer	14x14, 512
19	MaxPooling2D Layer	7x7, 512
20	Flatten layer	25088 parameters
21	Dense Layer	6422784 parameters
22	Dropout Layer	Dropout=0.3
23	Dense Layer(Output Layer)	4 classes

IV. RESULTS AND DISCUSSION

In this section the data set utilized for the experiment is described with the system specification on which the model is implemented, then the result of the model is discussed.
A personal computer with 8 GB RAM with 1 TB hard disk of i7 processor with a graphic card was used for performing the experimentation using anaconda-navigator's Jupiter notebook for coding purpose.

In the proposed work the data division is standard i.e., 70-30 ratio. The experiment was carried out on the dataset which has 4 classes named CNV, DME, Drusen and Normal from Kaggle. Dataset distribution is shown in Table II.

TABLE II DATA DISTRIBUTION IN FOUR CLASSES

Classes	Train	Test	Validation	Total
CNV	11368	4872	8	16,248
DME	11348	4865	8	16,221
DRUSEN	8616	3489	8	12,113
NORMAL	11961	5126	8	17,095
TOTAL	43293	18352	32	61,677

The proposed method got the highest validation accuracy of 83.66% in 5 epochs. Early stopping is applied thus the model is saved with highest validation accuracy. Four matrices are used to evaluate the model named Accuracy, Validation Accuracy, Loss, Validation Loss. For the evaluation another model called Efficient Net is also implemented but it can't reach the accuracy of VGG-16. The Efficient Net model achieves only 81.20% accuracy. Table III illustrated the comparison of two models.

TABLE III COMPARISON OF TWO PROPOSED METHODS

Epoch	Parameters	1	2	3	4	5
VGG16	Accuracy	0.4757	0.6207	0.6370	0.7704	0.7749
	val_accuracy	0.7843	0.7335	0.6859	0.8366	0.7729
	Loss	1.6694	0.8790	0.8434	0.8184	0.8133
	val_loss	0.5448	0.6664	0.7764	0.4429	0.6642
EFFICIENT NET	Accuracy	0.4451	0.4431	0.4463	0.4456	0.4475
	val_accuracy	0.7500	0.7790	0.81208	0.8089	0.7904
	Loss	1.2315	1.2318	1.2301	1.2303	1.2269
	val_loss	2.1085	1.5445	0.9209	2.0631	1.7093

In the next table i.e., Table IV the output for each epoch and for each drop-out rate is shown. It is evaluated from the table that the model got how much accuracy and loss in which epoch**.** In the proposed model the size of the dataset is very huge thus the problem of over fitting increases. In first round the model is implemented with 25% dropout rate so the model is over fitted and gives the accuracy of 82.88%. Then in second round the dropout rate is set to 50% then the model is performed better and give accuracy of 83.66%. In last round the dropout rate is set to 75% the out corresponding to it is 82.08%.

TABLE IV DETAILED OUTPUT OF THREE DROP-OUT RATE

Model Name	Epoch	Loss	Accuracy	Val_Loss	Val_ Accuracy
Vgg-16 with 0.25 drop-out rate	1	0.6408	0.7553	0.7871	0.6681
	2	0.6300	0.7588	0.4644	0.7963
	3	0.6128	0.7648	0.4605	0.8288
	4	0.6065	0.7704	0.4562	0.8056
	5	0.6037	0.7749	0.4438	0.8264
Vgg-16 with 0.50 drop-out rate	1	1.6694	0.4757	0.5448	0.7843
	2	0.8790	0.6207	0.6664	0.7335
	3	0.8434	0.6370	0.7764	0.6859
	4	0.8184	0.7704	0.4429	0.8366
	5	0.8133	0.7749	0.6642	0.7729
Vgg-16 with 0.75 drop-out rate	1	1.6086	0.3095	0.8855	0.8208
	2	1.3280	0.3332	0.8734	0.8026
	3	1.3277	0.3303	0.9496	0.7581
	4	1.3257	0.3303	1.0118	0.7295
	5	1.3228	0.3363	0.9924	0.7223

For VGG-16 the model is executed for three times for different Drop-out rate so that the evaluation of the model can be done in a better way. With each drop-out rate model got different validation-accuracy. In Table V the evaluation is shown in a aggregate manner. This can be understood that with less drop-out rate the validation accuracy improves but it may be because of the over fitting of the model, thus for reducing the over fitting the drop-out rate is increased. But it is observed that the moderate drop-out rate e.g., 0.50 is better because it achieves the accuracy of 83.66% which is not due to over fitting.

TABLE V COMPARISON OF THREE DROP-OUT RATE

Drop-out Rate	Highest Validation Accuracy	Lowest Validation Loss	In Epoch
0.25	0.8288	0.4605	3
0.50	0.8366	0.4429	4
0.75	0.8208	0.8855	1

The output of the proposed method can be visualized in fig 4. The validation loss is dropped at very high rate and the validation accuracy is decreased first then it increased gradually. The accuracy and loss for the training images are almost constant.

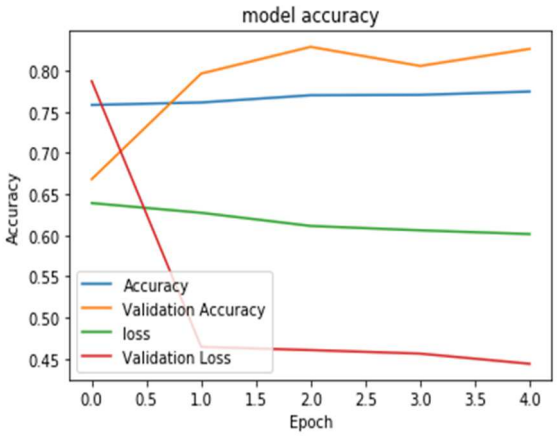

(a)

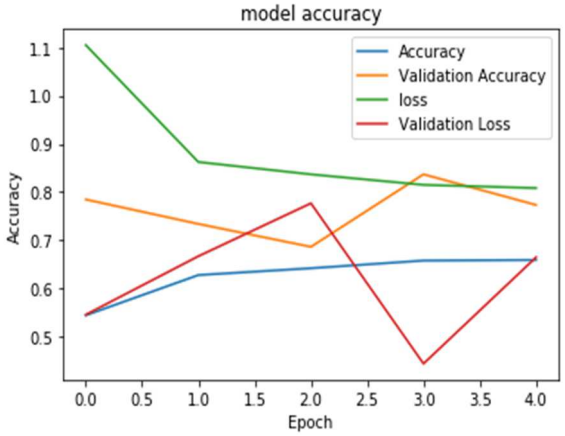

(b)

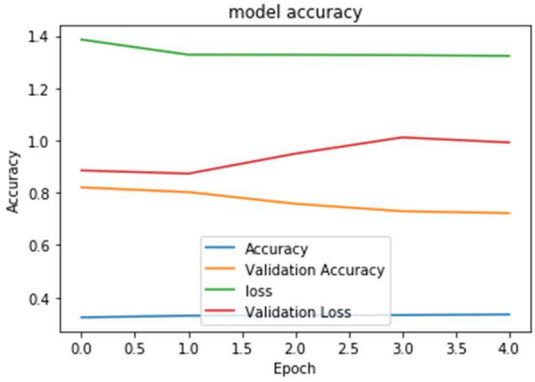

(c)

Fig-4 Graph For The Proposed Method (A) Drop-Out Rate-0.25(B) Drop-Out Rate-0.50(C) Drop-Out Rate-0.75

After this execution the testing data set is reduced to the level of Sivamurugan Vellakani et. Al. [16] so that a comparison can be showcase in the results.

The distribution of data is shown in Table VI.
In the proposed model the size of the dataset is very huge thus the problem of over fitting increases. In first round the model is implemented with 25% dropout rate so the model is over fitted and gives the accuracy of 99.66%. Then in second round the dropout rate is set to 50% then the model is performed better and give accuracy of 97.3%. In last round the dropout rate is set to 75% the out corresponding to it is 95.33%.

TABLE VI DATA DISTRIBUTION IN FOUR CLASSES

Classes	Train	Test	Validation	Total
CNV	11368	242	8	11618
DME	11348	234	8	11590
DRUSEN	8616	242	8	8866
NORMAL	11961	242	8	12211
TOTAL	43293	960	32	44285

The proposed method got the highest validation accuracy of 99.00% in 5 epochs. Early stopping is applied thus the model is saved with highest validation accuracy. Four matrices are used to evaluate the model named Accuracy, Validation Accuracy, Loss, Validation Loss. For the evaluation another model called Efficient Net is also implemented but it can't reach the accuracy of VGG-16. The Efficient Net model achieves only 81.20% accuracy. Table VII illustrated the comparison of two models.

TABLE VII COMPARISON OF TWO PROPOSED METHODS

Epoch	Parameters	1	2	3	4	5
VGG16	accuracy	0.5575	0.7205	0.7460	0.7576	0.7658
	val_accuracy	0.8900	0.8933	0.9300	0.9167	0.9900
	Loss	0.5006	0.7067	0.6594	0.6324	0.6175
	val_loss	0.2829	0.3514	0.1892	0.2664	0.1407
EFFICIENT NET	accuracy	0.4451	0.4431	0.4463	0.4456	0.4475
	val_accuracy	0.7500	0.7790	0.81208	0.8089	0.7904
	Loss	1.2315	1.2318	1.2301	1.2303	1.2269
	val_loss	2.1085	1.5445	0.9209	2.0631	1.7093

In the next table i.e. Table VIII the output for each epoch and for each drop-out rate is shown. It is evaluated from the table that the model got how much accuracy and loss in which epoch.

TABLE VIII DETAILED OUTPUT OF THREE DROP-OUT RATE

Model Name	Epoch	Loss	Accuracy	Val_Loss	Val_ Accuracy
Vgg-16 with 0.25 drop-out rate	1	1.5006	0.5575	0.2829	0.8900
	2	0.7067	0.7205	0.3514	0.8933
	3	0.6594	0.7460	0.1892	0.9300
	4	0.6324	0.7576	0.2664	0.9167
	5	0.6175	0.7658	0.1407	0.9900
Vgg-16 with 0.50 drop-out rate	1	0.9512	0.5931	0.3174	0.9533
	2	0.9178	0.6076	0.2352	0.9733
	3	0.9009	0.6079	0.3591	0.9267
	4	0.8960	0.6127	0.3086	0.9467
	5	0.8760	0.6216	0.2595	0.9567
Vgg-16 with 0.75 drop-out rate	1	1.7218	0.2864	0.9019	0.8033
	2	1.2975	0.3305	0.8458	0.8067
	3	1.2908	0.3285	0.7133	0.8367
	4	1.2946	0.3268	0.6791	0.8500
	5	1.2865	0.3386	0.6365	0.9533

For VGG-16 the model is executed for three times for different Drop-out rate so that the evaluation of the model can be done in a better way. With each drop-out rate model got different validation-accuracy. In Table IX the evaluation is shown in an aggregate manner. This can be understood that with less drop-out rate the validation accuracy improves but it may be because of the over fitting of the model, thus for reducing the over fitting the drop-out rate is increased. But it is observed that the moderate drop-out rate e.g., 0.50 is better because it achieves the accuracy of 97.33% which is not due to over fitting.

TABLE IX COMPARISON OF THREE DROP-OUT RATE

Drop-out Rate	Highest Validation Accuracy	Lowest Validation Loss	In Epoch
0.25	0.9900	0.1407	5
0.50	0.9733	0.2352	2
0.75	0.9533	0.6365	5

The output of the proposed method can be visualized in figure 5. The validation loss is dropped at very high rate and the validation accuracy is decreased first then it increased gradually. The accuracy and loss for the training images are almost constant

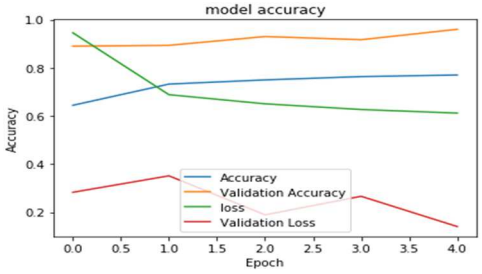

(a)

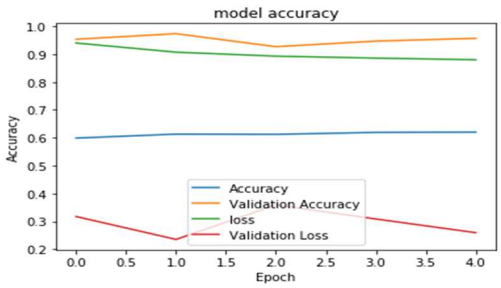

(b)

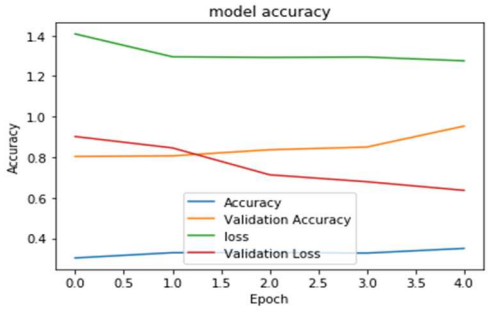

(c)

Fig-5 Graph for the proposed method (a) drop-out rate-0.25 (b) drop-out rate-0.50 (c) drop-out rate-0.75

V. COMPARATIVE ANALYSIS

For validation of the proposed model the comparison of this model is done with the model of Sivamurugan Vellakani et. Al. [16] model, they used CNN-LSTM model for the classification of diseases.

The proposed model achieves the accuracy 83.66% which is less than SivamuruganVellakani et. Al. [16] model's but the testing of the model is very rich as the shown in Table III. Then for validation the test data set is reduced to the level of SivamuruganVellakani et. Al. [16] and our proposed model achieve the overall accuracy 97.33% which is higher than they proposed. The visualization of the comparison of both models can be seen in Fig-6.

The proposed model is better than the model of SivamuruganVellakani et. Al. [16] because the data set is very rich, so the training of the model is very good and different dropout rates are applied for reducing the over fitting problem.

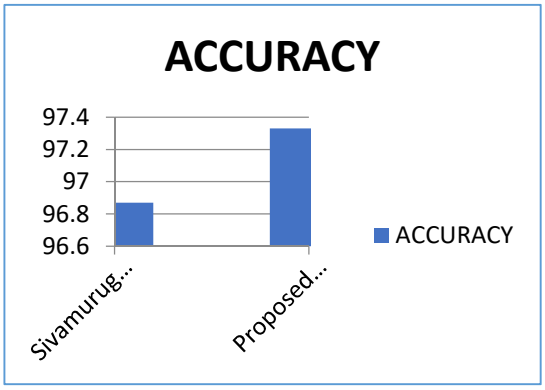

Fig-6 Comparison of proposed models and SivamuruganVellakani et. Al. [16] model

VI. Conclusion

Screening for CNV, DME and Drusen using Fundus photographs has already been widely used in all over the world. This methodology presents an efficient automated model for the detection of internal eye diseases in the OCT images of retina. The proposed methodology is performed on a huge OCT image data-set and the outcome indicates that the proposed model is efficient to detect the diseases. The model achieves the validation accuracy of 83.66% accuracy with 0.50 drop-out rate will be considered as the model accuracy with the standard data set. According to the performance metrics, the performance of VGG-16 is better, in prediction of the diseases like CNV, DME, Drusen. Thus, it can be utilized for the assistance of the ophthalmologist. Future work includes the implementation of automated model for the detection of the other eye diseases or external eye diseases with the higher accuracy which is achieved in this model.

References

1. Alan D. Fleming, Sam Philip, Keith A. Goatman, John A. Olson, and Peter F. Sharp, "Automated microaneurysm detection using local contrast normalization and local vessel detection," IEEE TRANSACTIONS ON MEDICAL IMAGING, VOL. 25, NO. 9, SEPTEMBER 2006.
2. Arturo Aquino, Manuel Emilio Gegúndez-Arias, and Diego Marín,"Detecting the optic disc boundary in digital fundus images using morphological, edge detection, and feature extraction techniques," IEEE TRANSACTIONS ON MEDICAL IMAGING, VOL. 29, NO. 11, NOVEMBER 2010.
3. Gwénolé Quellec, Stephen R. Russell, and Michael D. Abràmoff , "Optimal filter framework for automated, instantaneous detection of lesions in retinal images," IEEE TRANSACTIONS ON MEDICAL IMAGING, VOL. 30, NO. 2, FEBRUARY 2011.
4. Jun Cheng, Dacheng Tao, Jiang Liu,Damon Wing Kee Wong, Ngan-Meng Tan, Tien Yin Wong, and Seang Mei Saw, "Peripapillary atrophy detection by sparse biologically inspired feature manifold," IEEE TRANSACTIONS ON MEDICAL IMAGING, VOL. 31, NO. 12, DECEMBER 2012.
5. Jun Cheng, Jiang Liu, Yanwu Xu, Fengshou Yin, Damon Wing Kee Wong, Ngan-Meng Tan, Dacheng Tao, Ching-Yu Cheng, Tin Aung, and Tien Yin Wong ,"Superpixel classification based optic disc and optic cup segmentation for glaucoma screening," IEEE TRANSACTIONS ON MEDICAL IMAGING, VOL. 32, NO. 6, JUNE 2013.
6. Uyen T. V. Nguyen, Alauddin Bhuiyan, Laurence A. F. Park, Ryo Kawasaki, Tien Y. Wong, Jie Jin Wang, Paul Mitchell, and Kotagiri Ramamohanarao, An Automated Method for Retinal Arteriovenous Nicking Quantification From Color Fundus Images , IEEE TRANSACTIONS ON BIOMEDICAL ENGINEERING, VOL. 60, NO. 11, NOVEMBER 2013.
7. Stuart Keel, Jinrong Wu, Pei Ying Lee, Jane Scheetz, Mingguang He, Visualizing Deep Learning Models for the Detection of Referable Diabetic Retinopathy and Glaucoma, JAMA Ophthalmol. 2019;137(3):288-292. doi:10.1001/jamaophthalmol.2018.6035 Published online December 20, 2018.
8. Ursula Schmidt-Erfurth Hrvoje Bogunović , Amir Sadeghipour , Bianca S. Gerendas , Sebastian M. Waldstein, Artificial intelligence in retina, Retinal and Eye Research 67 (2018) 1–29, Published by Elsevier Ltd.
9. Yifan Peng, Shazia Dharssi, Qingyu Chen, Tiarnan D. Keenan, Elvira Agrón, Wai T. Wong, Emily Y. Chew, Zhiyong Lu, Deepseenet, a deep learning model for automated classification of patient based age-related macular degeneration severity from color fundus photographs, 2018 by the American Academy of Ophthalmology Published by Elsevier Inc.
10. Liu Li, Mai Xu, Hanruo Liu, Yang Li, Xiaofei Wang, Lai Jiang, Zulin Wang, Xiang Fan, and Ningli Wang, A large-scale database and a cnn model for attention-based glaucoma Detection, IEEE TRANSACTIONS ON MEDICAL IMAGING,2019.
11. Xue-Bi Cai , Shou-Ren Shen , De-Fu Chen , Qingjiong Zhang , Zi-Bing Jin , An overview of myopia genetics, Experimental Eye Research 188 (2019) 107778.
12. Carol Y. Cheung, Fangyao Tang, Daniel Shu Wei Ting, Gavin Siew Wei Tan and Tien Yin Wong, Artificial intelligence in diabetic eye disease screening ,Asia-Pacific Journal Of Ophthalmology • Volume 8, Number 2, March/April 2019.
13. Janelle Tong, Jack Phu, Michael Kalloniatis, And Barbara Zangerl, Modeling changes in corneal parameters with age, Implications for Corneal Disease Detection, PUBLISHED BY ELSEVIER INC .0002-9394.
14. Muhammad Aamir , Muhammad Irfan, Tariq Ali, Ghulam Ali , Ahmad Shaf , Alqahtani Saeed S, Ali Al-Beshri , Tariq Alasbali and Mater H. Mahnashi, An adoptive threshold-based multi-level deep convolutional neural network for glaucoma eye disease detection and classification, Diagnostics 2020, 10, 602; doi:10.3390/diagnostics10080602.
15. Thippa Reddy Gadekallu, Neelu Khare, Sweta Bhattacharya, Saurabh Singh, Praveen Kumar Reddy Maddikunta, In-Ho Ra and Mamoun Alazab, Early detection of diabetic retinopathy using pca-firefly based deep learning model, Electronics 2020, 9, 274; doi:10.3390/electronics9020274.
16. Sivamurugan Vellakani and Indumathi Pushbam , An enhanced OCT image captioning system to assist ophthalmologists detecting and classifying eye diseases, Journal of X-Ray Science and Technology xx (20xx) x–xx ,DOI 10.3233/XST-200697.
17. Philipp Seeböck , Sebastian M. Waldstein, Sophie Klimscha, Hrvoje Bogunovic , Thomas Schlegl,Bianca S. Gerendas, René Donner, Ursula Schmidt-Erfurth, and Georg Langs, Unsupervised identification of disease marker candidates in retinal oct imaging data, IEEE TRANSACTIONS ON MEDICAL IMAGING, VOL. 38, NO. 4, APRIL 2019.
18. Philipp Seeböck, José Ignacio Orlando, Thomas Schlegl, Sebastian M. Waldstein, Hrvoje Bogunović,Sophie Klimscha, Georg Langs, and Ursula Schmidt-Erfurth, Exploiting epistemic uncertainty of anatomy segmentation for anomaly detection in retinal OCT, IEEE TRANSACTIONS ON MEDICAL IMAGING, VOL. XX, NO. XX, MAY 2019.
19. Kenneth W. Tobin, Senior Member, Edward Chaum, V. Priya Govindasamy, Member and Thomas P. Karnowski, Detection of anatomic structures in human retinal imagery, IEEE TRANSACTIONS ON MEDICAL IMAGING, VOL. 26, NO. 12, DECEMBER 2007.
20. Qassim, H., Verma, A., & Feinzimer, D.,Compressed residual-VGG16 CNN model for big data places image recognition, In 2018 IEEE 8th Annual Computing and Communication Workshop and Conference (CCWC) (pp. 169-175). IEEE, 2018, January.
21. Kaur, T., & Gandhi, T. K., Automated brain image classification based on VGG-16 and transfer learning, In 2019 International Conference on Information Technology (ICIT) (pp. 94-98). IEEE, 2019, December.
22. Dodge, S., & Karam, L., Understanding how image quality affects deep neural networks. In 2016 eighth international conference on quality of multimedia experience (QoMEX) (pp. 1-6). IEEE, 2016, June.
23. Liu, S., & Deng, W.,Very deep convolutional neural network based image classification using small training sample size. In 2015 3rd IAPR Asian conference on pattern recognition (ACPR) (pp. 730-734). IEEE, 2015, November.
24. https://medium.com/towards-artificial-intelligence/the-architecture-and-implementation-of-vgg-16-b050e5a5920b